2005

The Effects of β-Mercaptoethanol on the Specific Activity of Porphobilinogen Synthase Mutants of the Rhodobacter sphaeroides Protein

Trefan Archibald '05
Illinois Wesleyan University

The Effects of β-Mercaptoethanol on the Specific Activity of Porphobilinogen Synthase Mutants of the *Rhodobacter sphaeroides* Protein.

Trefan Archibald

David W. Bollivar, Ph.D., Faculty Advisor

Thesis for Biology 499 and Research Honors: 2004-2005

Illinois Wesleyan University

TABLE OF CONTENTS

ABSTRACT

The enzyme porphobilinogen synthase (PBGS) catalyzes the conversion of two molecules of δ-aminolevulinic acid (ALA) into porphobilinogen (PBG) in the first common step of the tetrapyrrole biosynthesis pathway.[10] A homology model of the *R. sphaeroides* PBGS was created by Dr. Eileen K. Jaffe at Fox Chase Cancer Center based on comparison to the crystal structure of *Pseudomonas aeruginosa.* The proposed structure suggests that there are four cysteines in close proximity to the active site. Three of these cysteines are not present in the highly similar *R. capsulatus* sequence.[1] Under oxidizing conditions these residues can potentially participate in the formation of disulfide bonds, which would be potential targets for reducing agents, such as β-mercaptoethanol. This is supported by the fact that a number of PBGS enzymes require the addition of β-mercaptoethanol for full activity, including the *Rhodobacter sphaeroides* enzyme. To test if the three cysteines that are present in the *R. sphaeroides* enzyme, and not that of *R. capsulatus,* are responsible for the dependence of *R. sphaeroides* on a reducing agent (β-mercaptoethanol), site-directed mutagenesis was performed on *R. sphaeroides*. After the presence of the mutations was confirmed through sequencing, the altered enzymes were isolated and tested for β-mercaptoethanol sensitivity. A decrease in sensitivity is found in all three mutants when compared to wild type. In two mutants of these mutants, C103D and C265V, the difference is very pronounced. A larger goal was to test whether the current structural model is sufficient to serve as a guide for further work on the structure-function relationships in the *R. sphaeroides* PBGS. Our results indicate that the system is more complicated than anticipated. Further study is needed to clarify the role of cysteine residues.

INTRODUCTION AND THEORY

PBG Background

Porphobilinogen (PBG), illustrated in Scheme 1[6], the monopyrrole product of the reaction catalyzed by PBGS, is a precursor to all biological tetrapyrroles.[11] Tetrapyrroles are four-membered heteronuclear rings that include some of the most widely present and important compounds in nature. All chlorophylls and hemes, vitamin B_{12}, and Factor 430 are among the most notable compounds that are tetrapyrroles (Figure 2).[11] Thus production of PBG, which is the first common step in the biosynthesis of all tetrapyrrole products, is integral to sustainting life. Understanding asymmetric condensation of two molecules of δ-aminolevulinic acid (ALA) to give one molecule of PBG will provide much insight into the exciting possibilities for future clinical applications such as rational drug design and toxicology. Since this reaction is enzyme catalyzed, it would be advantageous for us to understand the mechanism by which PBGS works.

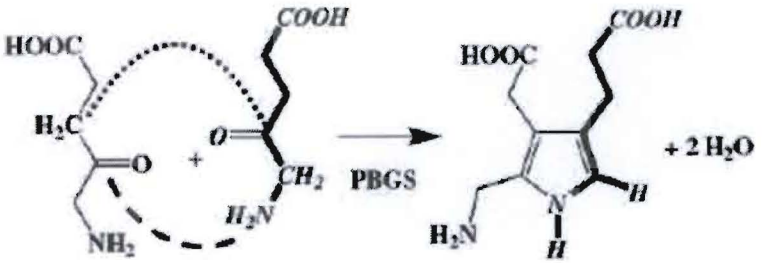

A-Site ALA P-Site ALA PBG

Scheme 1. Balanced reaction catalyzed by PBGS. The conversion of two molecules of δ-aminolevulinic acid to one molecule of porphobilinogen and two molecules of water. The P-site substrate molecule, and what it contributes to the porphobilinogen, is in bold. The A-site substrate molecule, and what it contributes to the porphobilinogen, is not in bold[6].

PBGS Mechanism

The metalloenzyme, PBGS, catalyzes the biosynthesis of PBG from two molecules of δ-aminolevulinic acid, which is thought to occur via a Knorr type pyrrole condensation[10]. The mechanism is fairly well supported through intermediate analog studies and generally accepted (mechanism in Scheme 3[11] and intermediate analogs in Figure 6[3, 6]).[3, 6, 9, 10, 11] One molecule of δ-aminolevulinic acid enters the active site of the enzyme. The acid forms a Schiff base with an active site lysine residue at the P-Site, which is so named because the substrate molecule that binds to this site contributes the propanoic acid side chain to porphobilinogen. Then a second molecule of substrate forms

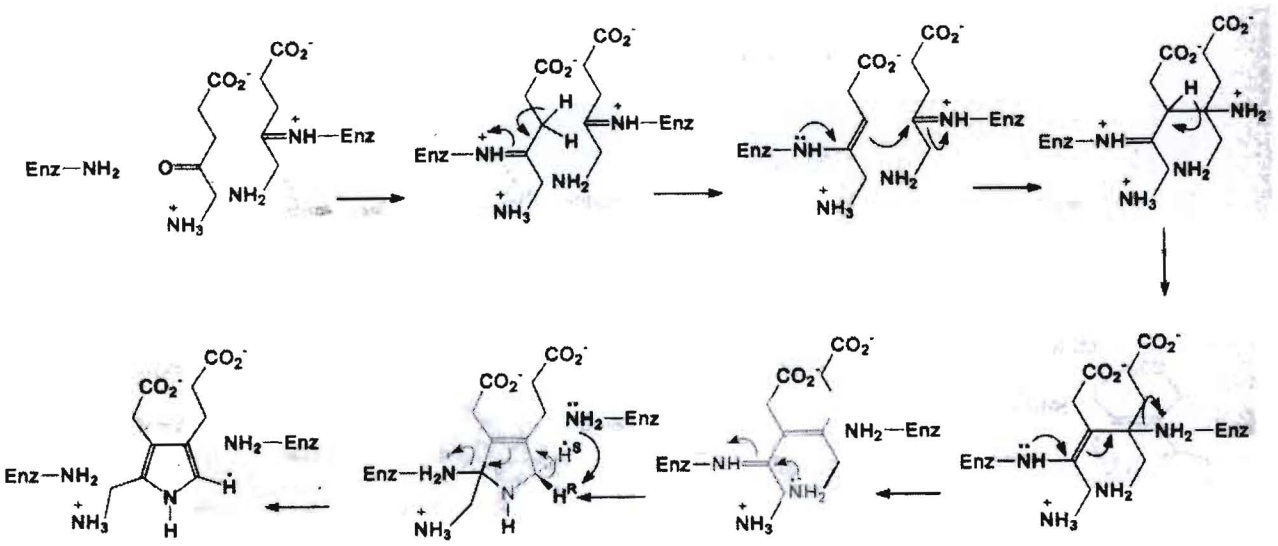

Scheme 3. Mechanism proposed for porphobilinogen synthesis proposed by Jordan et. al. Both substrate molecules are bound to enzyme through Schiff bases and C-C bond is the first one formed[11].

another Schiff base with a lysine residue in the A-site part of the active site, so named because the substrate molecule that binds to this site contributes the acetic acid side chain to the porphobilinogen. The substrate molecule at the A-site then loses a proton from the three position and an aldol condensation occurs. This causes a nucleophilic attack by the 3 position carbon on the A-site substrate molecule on the carbon of the Schiff base of the P-site substrate molecule. The second proton is then lost from the three carbon on the A-site substrate molecule and a second aldol condensation occurs. The intermediate then detaches from the P-site. The P-site amino group then nucleophilically attacks the Schiff base on the A-site substrate molecule. Then another deprotonation occurs and the newly synthesized porphobilinogen molecule detaches from the A-site.

There is still some debate over this mechanism.[11] First, there is no evidence that suggests that the formation of the C-C bond preceeds C-N bond formation An alternative mechanism in which C-N bond first is shown in Scheme 4.[11] The only reason the C-N bond is not thought to form first is that this mechanism would cause electrosteric hinderance for the subsequent C-C bond formation. Also, there is no definitive experiment demonstrating that there is a Schiff Base formed at the A-site, mechanism shown in Scheme 5.[11] The only evidence that indicates this second Schiff Base comes from an intermediate analog study.[6] This study revealed that intermediate analog, 4,7-dioxosebasic acid (Figure 6), was covalently reacted with two lysine residues. However, whether this compound is a true analog of the porphobilinogen was not determined.

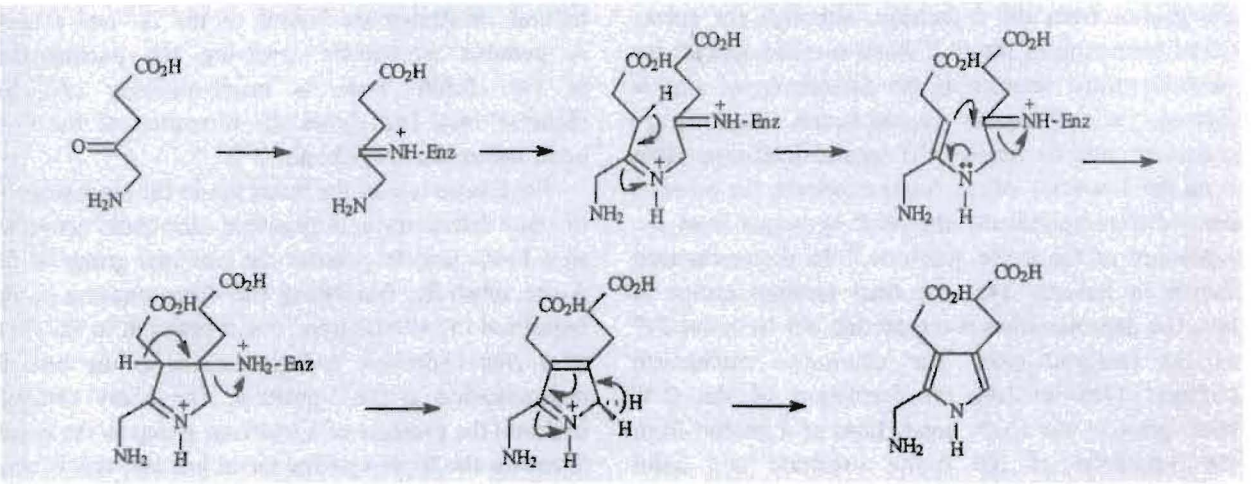

Scheme 4. Alternate mechanism proposed for porphobilinogen synthesis. Only one of the substrate molecules are bound to enzyme through a Schiff base and the C-N bond is the first one formed[11].

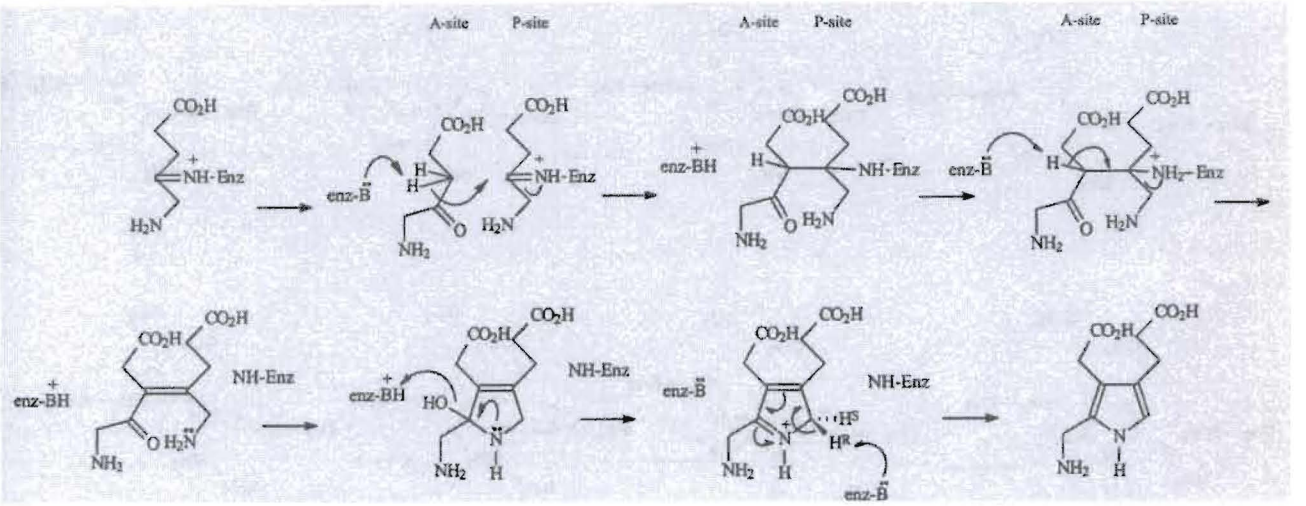

Scheme 5. Alternate mechanism proposed for porphobilinogen synthesis. Only one of the substrate molecules are bound to enzyme through Schiff bases and the C-C bond is the first one formed[11].

Active Site

There are two classifications of PBGS enzymes (Figure 13[4]).[4] The first classification is variation in active site metal ion binding. The metal ion used most is zinc, which is always in the +2 ionization state, Figure 14.[4] The use of catalytic zinc can be explained in two ways. First, the transition metal does not discriminate between different first coordinate sphere ligands or ligation geometry. Also, zinc is fairly ubiquitous in most environments. Mg(II) and/or potassium(I) can also occupy this role. Mg(II) is thought to be used less because the alkaline earth metal prefers binding oxygen ligands in a rigid octahedral geometry. The binding of K(I) shows that charge is not the only determinant of function. The use of monovalent cations indicate further malleability because monovalent cations can usually accommodate more ligands. Of all know PBGS

sequences, there seems to be an even split between having the determinants for zinc binding and having the determinants for magnesium and/or potassium binding. For those enzymes that have a catalytic zinc, a consensus binding motif has been assembled as DXCXCX(Y/F)X_3G(H/Q)CG, where the coordination cysteines are underlined and X has limited variability. However, in non-zinc binding PBGS enzymes, the active site metal binding sequence has been formed as DXALDX(Y/F) X_3G(H/Q)DG. In this aspartate rich sequence, the underlined aspartic acid residues underlined are thought to coordinate the magnesium and/or potassium.

Allosteric Site

The second classification is based on allosteric site metal binding.[4] The magnesium(still +2) is thought to stabilize the monomer interactions. The complexity of active site metals is in stark contrast to the simplicity of allosteric site metal binding. PBGS enzymes either has an allosteric magnesium (still +2) at this site, an example is shown in Figure 15[4], or binds nothing at all but still has a consensus sequence. Over 90% of all known PBGS sequences contain the determinants for the allosteric magnesium binding site. This consensus sequence is $RX_{\sim 164}DX_{\sim 65}EXXXD$. Also, a non-magnesium binding allosteric site consensus sequence has been outlined as $XX_{\sim 164}DX_{\sim 65}XXXRD$.

Clinical Significance

The biological importance of derivatives of the products of the reaction that involves condensation of two molecules of δ-aminolevulinic acid into one porphobilinogen molecule leads to many clinical implications for the PBGS enzyme. PBGS has long been known to be the target of lead poisoning in humans.[5, 7, 13] However,

the absence of a mechanism has hindered progress for clinical treatments. A recent paper by Jaffe et. al. proposed a mechanism through which Pb(II) inhibits PBGS activity.[5] Human PBGS is a metalloenzyme that coordinates Zn(II) with cysteine residues. There appear to be two distinct types of zinc binding site, named ZnA and ZnB (Figure 7[5]). This study shows that both of these sites bind preferentially to Pb(II) and the ZnA site is responsible for slow, tight binding of Pb(II). Their data supports Pb(II) binding to a hybrid site which uses ligands from both the ZnA and ZnB sites, shown in Figure 8B[5], however does not fully exclude the Pb(II) binding to only the ZnB ligands, shown in figure Figure 8A.[5] This Pb(II) binding is proposed to be disfavored during turnover because of the lone pair of electrons on Pb(II) which would alter the active site microenvironment thereby decreasing substrate binding and the ensuing catalysis of the reaction.

Designer bioselective inhibitor production is also an exciting clinical possibility.[12] In the past, searches for antibiotics, fungicides, herbicides, etc. have been based either solely upon trial and error method or a novel observation. With today's molecular knowledge, this process can be streamlined by removing much of the randomness of the search. This could be done by exploiting the differences in necessary enzymatic activities between host and parasite. PBGS seems to be an optimal system in which to do this because it is nearly omnipresent in the biotic world. Theoretically, when the human PBGS and a given infectious organism PBGS have been sufficiently characterized, differences in active and allosteric sites could be utilized to determine the attributes that a compound should hypothetically have to selectively disrupt the infectious agent. From here, chemical databanks could be searched or *de novo* synthesis could be used to

formulate a list of possible selectively disruptive agents. Then testing for the clinical effectiveness and toxicity of each compound would all that remained to do.

PBGS Structure

Of the over 130 sequenced PBGS enzymes, there are only X-ray crystallography structures for four species: yeast, *E. coli*, *Pseudomonas aeruginosa*, and human. A homo-octameric structure is conserved (Figure 9B[8]), however active site ligands vary (Figure 10[4]).[4] Each monomer is composed an αβ barrel, which contains the active site and an N-terminal arm (Figure 11[11]). The N-terminal arm is involved in subunit-subunit interactions. It is thought that the arm of one subunit "hugs" the barrel of the other subunit of the dimmer. These dimers then assemble, through hydrophobic interactions, in to the "69" confirmation (Figure 9A[8]). Then four dimers assemble into an octamer in the D4 confirmation (Figure 9B[8]). Since eight spatially distinct but structurally equivalent subunits are identified through X-ray structures, it is reasonable to assume that there are eight active sites per enzyme. However there is evidence that there are only four active sites per homo-octamer in both mammalian and *E. coli* PBGS.[2] This supports the theory that PBGS has half-site reactivity. Recently, a breakthrough experiment with *Rhodobacter capsulatus* that used both size-exclusion chromatography and analytical ultracentrifugation indicates that this organism's PBGS enzyme can be predominantly found in a very active hexameric state.[1] Also, another recent study shows that a rare human allele for PBGS, F12L, causes an oligomeric switch where the octamer is changed to a hexamer which no longer bind an allosteric magnesium (Figure 12[2]).[2] This is thought to destabilize the normal, or Mg^{+2}-stabilized hugging dimer, making it easier to

take on a different dimer confirmation, called detached dimer. This detached dimer can form a hexamer. This conversion between oligomeric states is hypothesized to be part of allosteric regulation of PBGS because there is also a marked change in pH rate profile. The variant has optimal K_m and V_{max} at pH 9 in contrast to wild type, which has an optimal pH of 7. So *in vivo*, the hexamer has about 12% of the activity that the wild type does. Thus shifts in the oligomeric state equilibrium would be predicted to alter the overall PBGS activity *in vivo* and perhaps play a role in tetrapyrrole biosynthesis regulation.

OBJECTIVE

The immediate goal of this study is to test whether the fact that the wild type *R. sphaeroides* PBGS activiy is dependent upon β-mercaptoethanol is due to disulfide bonds involving the three cysteine residues in close proximity to the active site (Figure 16). These disulfide bonds would necessitate a reducing environment to keep from oxidizing, changing the structure and possibly the activity of PBGS.

The overall goal of this study is to test whether the structural model that has been prepared is sufficiently accurate to serve as a guide for further experiments on structure-function relationships in the PBGS enzyme in *R. sphaeroides.* Further understanding structure and function will facilitate creating clinical applications. Also, in respect to the field of PBGS study in a whole, we would like to contribute to the amassing library of knowledge. This will allow future work to use a comparative method and take advantage on natural phylogenetic variations in the enzyme to facilitate future work.

RESULTS AND DISCUSSION

The cysteine residues mutated were chosen because these cysteins are present in *R. sphaeroides* PBGS and not that of *R. capsulatus,* which has high sequence homology with the *R. sphaeroides* PBGS(Figure 16). The significance of their presence only in the *R. sphaeroides* enzyme is that the *R. sphaeroides* enzyme is stimulated by β-mercaptoethanol and the *R. capsulatus* enzyme is not. Thus, it was hypothesized that one of these three cysteine residues present only in the *R. sphaeroides* PBGS participates in a disulfide bond and creates the dependence of the *R. sphaeroides* PBGS on the reducing agent β-mercaptoethanol. Also, since the justification of mutant choice was based on the homology between the *R. sphaeroides* and *R. capsulatus* PBGS, the residues mutated in the *R. sphaeroides* enzyme were changed to the amino acid found in the corresponding position in the *R. capsulatus* enzyme.

Sequencing was sent to MWG Bioscience. Alignments were then made between each mutant nucleotide sequence and wild type nucleotide sequence (Figure 19 and 20). The sequencing confirmed mutants C103D and C265V, however MWG was unable to sequence the C309A mutant. There is evidence to support the creation of C309A though. The C309A PBGS is stimulated markedly less by β-mercaptoethanol than the wild type PBGS. This supports the mutation of a disulfide participating cysteine residue to a non-disulfide participating amino acid residue.

The PBGS activity assays were run and the change in absorbance at 555 nm was used to determine enzymatic activity. To determine total protein concentration, Bradford assays were run and the change in absorbance at 595 nm was taken. Specific activity, which is essentially a measure of sample purity, of each assay was then calculated by

dividing the PBGS enzymatic activity by the total protein concentration. Then the specific activities of each sample in the presence and absence of β-mercaptoethanol were compared against each other(Figure 17 and 18). The specific activities of all the mutants were not as drastically decreased by the absence of β-mercaptoethanol as was the wild type. However, the specific activity of mutant C309A was stimulated markedly more than either mutant C103D or mutant C265V, and thus had enzymatic activity more similar to that of the wild type. Also, mutant C265V has low specific activity across the board which indicates that this cysteine may be an important residue.

For the purpose of this study, the simplest system that could exist would be one where the PBGS of *R. sphaeroides* has only one disulfide bond. The results that we would expect from this enzyme would be a total lack of stimulation by β-mercaptoethanol in mutant enzymes that contained amino acid changes at any cysteine residue that participated in the disulfide bond. In this theoretical system, at most two of the cysteine residues tested could participate in the disulfide bond and therefore only two of the tested mutants would lack any stimulation by β-mercaptoethanol. However, this is not what was observed. All three mutants were stimulated to some degree but none of the mutations were stimulated as much as the wild type. Mutant C103D PBGS has high overall activity and little stimulation by β-mercaptoethanol when compared to the wild type PBGS. The lack of stimulation suggests that this cysteine residue does participate in a disulfide bond. Also, the retention of a relatively high specific activity indicates that this mutated residue was not otherwise important to the function of the active site. Mutant C265V also had little stimulation by β-mercaptoethanol, but this mutant enzyme did not retain a relatively high specific activity. The overall loss of activity suggests that

this cysteine residue is important to the function of the active site in addition to possibly participating in a disulfide bond. The last mutant, C309A, retained high specific activity, however it showed more considerable stimulation by β-mercaptoethanol. With this evidence, it is hard to suggest that the residue does or does not participate in a disulfide bond.

FUTURE WORK

First and foremost, more extensive mutations of cysteine residues need to be made and evaluated. For safe measure, the fourth cysteine residue at position 315 in Figure 16, which is present in both *Rhodobacter* species, (Figure 16) should be mutated and evaluated. That work should be followed by making various combinations of cysteine residues to determine exactly which residues were interacting in each disulfide bond.

Then reciprocal mutations should be made in *R. capsulatus* by changing amino acid residues to cysteines at corresponding positions to the mutations made in *R. sphaeroides* PBGS. These mutants should then be confirmed, purified, and tested for β-mercaptoethanol sensitivity. If the reciprocal mutations in *R. capsulatus* imparted β-mercaptoethanol sensitivity, then this would further confirm that cysteine residues in *R. sphaeroides* are participating in structurally and functionally important disulfide bonds.

METHODS AND MATERIALS

Mutagenesis

Mutagenesis was carried out with Stratagene QuickChange Site-Directed Mutagenesis Kit. This was used to create three different mutants. The first was to change a cysteine residue to an aspartate at amino acid position 103. This mutant will be referred to as C103D. Primers were 5'-ggcctggaaccccc**gac**aacctcgccaaccgg-3' and 5'-ccggttggcgaggtt**gtc**ggggttccaggcc-3' where the mutated residue is in bold. The second mutation was the change from a cysteine to a valine at amino acid residue at 265. This mutant will be referred to as C265V. Primers were 5'-ccctatctcgacatc**gtc**cggcgggtgaaggacgc-3' and 5'-gcgtccttcacccgccg**gac**gatgtcgagataggg-3'. The third mutant made was a cysteine to an alanine at residue 309. This mutant will be referred to as C309A. Primers were 5'-ccctatctcgacatc**gcc**cggcgggtgaaggacgc-3' and 5'-gcgtccttcacccgccg**ggc**gatgtcgagataggg-3' where the mutated residue is in bold.

Plasmid Purification

Mutant plasmid was transformed into XL1-Blue Supercompetent cells (from Stratagene). Then plasmid purification was carried out by QIAGEN-tip 100 Midiprep Kit.

Sequencing

Each purified plasmid (20 µl) was sent of to MWG Bioscience. Then alignments were created between the mutant sequences and the wild type sequence using NCBI Blast (Figures 19 and 20).

Mutant Protein Purification

The mutant and wild type plasmid wase transformed into BLR Supercompetent cells (Novagen), plated on LB with ampicillin and tetracycline and grown overnight at 37 °C. A single colony was then innoculated in 1 L LB with 0.4% glucose and 50mg/L of carbenicillin at 37 °C for 16 hours. The cells were spun down and pellets were resuspended for induction in 1 L of LB with 100 μM IPTG and 50 mg/L of carbenicillin at 15 °C for 24 hours. The cells were spun down and each pellet was resuspended in 20 ml of Lysis buffer (0.1 M Tris, 10 mM β-mercaptoethanol, 30 mM KCl, pH 8.5). The cells were then lysed using a French Press and treated with benzonuclease. Cellular debris was pelleted out with centrifugation at 21,500 x g and 4 °C for 15 minutes with a Beckman JLA-16.250 rotor. Ammonium sulfate precipitation was performed with the supernatant until ammonium sulfate was 25% saturation. To pellet the PBGS protein, centrifugation at 31,000 x g and 4 °C for 20 minutes with a Beckman JLA-16.250 rotor was performed. This pellet was then resuspended in 5 mL of Lysis buffer.

Wild Type Protein Purification

Purification of wild type protein follows all the steps included in the mutant protein purification but then is purified even further by three consecutive columns. After the ammonium sulfate precipitation pellet was resuspended in 5 ml of Lysis buffer, it was loaded on a HiPrep 16/10 Pheny FF phenyl sepharose column(Amersham-Pharmacia), which separates on degrees of hydrophobicity. The column was washed with Pheny Seph buffer A (30 mM Tris, 10 mM β-mercaptoethanol, pH 7) and eluted with a gradient from

Pheny Seph buffer A to Pheny Seph Buffer B (0.1 M Tris, 20% ammonium sulfate, 10 mM β-mercaptoethanol, pH 7). Fractions were collected and PBGS activity assays were run on the fractions. Fractions that showed high activity (OD of activity assay greater than 0.150) were pooled and loaded on a HiPrep 16/10 DEAE FF anion exchange column from Amersham-Pharmacia. The column was washed with DEAE buffer A (30 mM Tris, 10 mM β-mercaptoethanol, pH 7) and eluted with a gradient from DEAE buffer A to DEAE Buffer B (30 mM Tris, 0.6 M KCl, 10 mM β-mercaptoethanol, pH 7). Fractions were collected. These fractions were also assayed for PBGS activity and fractions of high activity were pooled. These pooled fractions were concentrated down to a 4 mL sample with Centricon centrifugal concentrators. This sample was then loaded on a HiPrep 26/60 Sephacryl S-300 size exclusion column from Ambersham-Pharmacia. The column was eluted with S-300 buffer (30 mM Tris, 30 mM KCL, 10 mM β-mercaptoethanol, pH 7). Fractions were collected and both activity assays and Bradford assays were run. The high specific activity showed successful purification. However, two activity peaks were observed and thus pooled separately. These two peaks might represent different oligomeric states, however no further tests were done to support this.

Assays

To determine enzymatic activity, five minute PBGS activity assays were run with all mutants and the wild type[10]. These assays were run in 0.1 M BTP pH 8.5 buffer in the presence of 30 mM KCl. These assays were carried out with and without the reducing agent, β-mercaptoethanol. Blanks were used as controls for all assays. The assays were then developed with Ehrlich's reagent and absorbance was taken at 555 nm.

For all samples Bradford assays were completed to determine total protein concentrations. Coomassie Protein Reagent (Pierce Chemical) was reacted with sample for 10 minutes then absorbance at 595 nm was taken and compared with a BSA standard curve to determine the protein content of each sample.

CONCLUSIONS

The lack of stimulation of C103D by the reducing agent and the maintenance of relatively high specific activity suggests that this cysteine participates in a disulfide bond. The loss of high specific activity in the C265V mutant obscures whatever the results might have been and thus we can draw no conclusions to whether this cysteine participates in a disulfide bond. However, the general lowering of specific activity suggests that this cysteine residue is otherwise important to the enzymes activity. The mutant C309A is still substantially stimulated by the reducing agent but not as stimulated as the wild type PBGS. This makes it difficult to draw any type of conclusions on the potential participation of this cysteine residue in a disulfide bond.

ACKNOWLEGMENTS

Thanks to David W. Bollivar, Ph.D., my thesis advisor, who knew when to guide me and when to let me learn from my mistakes and who tirelessly helped me edit my thesis.

Also, thanks to Laura Cathelyn who helped run assays during the protein purification in exchange for some samples and some guidance.

REFERENCES

1. Bollivar, D., Clauson, C., Lighthall, R., Forbes, S., Kokona, B., Fairman, R., Kundrat, L., Jaffe, E. Rhodobacter capsulatus porphobilinogen synthase, a high activity metal ion independent hexamer. *BMC Biochemistry.* 5:17, **2004.**

2. Breinig, S., Kervinen, J., Stith, L., Wasson, A., Fairman, R., Wlodawer, A., Zdanov, A., Jaffe, E. Control of tetrapyrrole biosynthesis by alternate quaternary forms of porphobilinogen synthase. *Nature Structural Biology.* 10(9): 757-763, **2003.**

3. Frere F, Schubert W, Stauffer F, Frankenberg N, Jahn R, Neier D, Heinz D: Structure of Porphobilinogen Synthase from Pseudomonas Aeruginosa in Complex with 5-Fluorolevulinic Acid Suggests a Double Schiff Base Mechanism. *J. Mol Biol.*, 320:237, **2002.**

4. Jaffe, E.K. An unusual phylogenetic variation in the metal ion binding sites of porphobilinogen synthase. *Chem. Biol.* 10: 25-34, **2003.**

5. Jaffe, E.K., Martins, J., Li, J., Kervinen, J., Dunbrack, R.L. Jr. The molecular mechanism of lead inhibition of human porphobilinogen synthase. *J. Biol. Chem.* 276(2): 1531-1537, **2001.**

6. Jaffe, E., Kervinen, J., Martins, J., Stauffer, F., Neier, R., Wlodawer, A., Zdanov, A. Species-specific inhibition of porphobilinogen synthase by 4-oxosebacic acid. *J. Biol. Chem.* 277(22): 19792-19799, **2002.**

7. Jaffe, E., Volin, M., Bronson-Mullins, C., Dunbrack, R. Jr., Kervinen, J., Martins, J., Quinlan, J. Jr., Sazinsky, M., Steinhouse, E., Yeung, A. An artificial gene for human porphobilinogen synthase allows comparison of an allelic variation

implicated in susceptibility to lead poisoning. *J. Biol. Chem.* 275(4): 2619-2626, **2000**.

8. Jaffe, E., unpublished

9. Mitchell, L., Volin, M., Martins, J., Jaffe, E. Mechanistic implications of mutations to the active site lysine of porphobilinogen synthase. *J. Biol. Chem.* 276(2): 1538-1544, **2001**.

10. Nandi DL, Baker-Cohen KF, Shemin D: Delta-aminolevulinic acid dehydratase of Rhodopseudomonas spheroides. *J. Biol Chem*, 243:1224-1230, **1968**.

11. Shoolingin-Jordan PM: The biosynthesis of Coproporphyrinogen III. *The Porphyrin Handbook. Volume 12*. Ed: Kadish KM, Smith KM and Guilard R. Amsterdam, Elsevier Science:33-74, **2003**.

12. Schoolingin-Jordan, P.M., Callahan, J.F.A., Cheung, K.M., Spencer,P., Warren, M.J.: Molecular diversity and selective targetting of enzymes in tetrapyrrole biosynthesis. *Phytochemical Diversity: A Source of New Industrial Products,* Cambridge, Royal Society of Chemistry, 115-128, **1997**.

13. Warren, M. J., Cooper, J. B., Woods, S. P. and Shoolingin-Jordan, P. M.: Lead poisoning, haem synthesis and 5-aminolaevulinic acid dehydratase. *Trends Biochem. Sci.* 23, 217-221, **1998**.

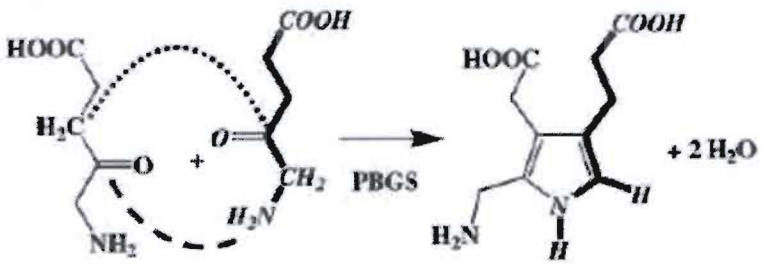

A-Site ALA P-Site ALA PBG

Scheme 1. Balanced reaction catalyzed by PBGS. The conversion of two molecules of δ-aminolevulinic acid to one molecule of porphobilinogen and two molecules of water. The P-site substrate molecule, and what it contributes to the porphobilinogen, is in bold. The A-site substrate molecule, and what it contributes to the porphobilinogen, is not in bold[6].

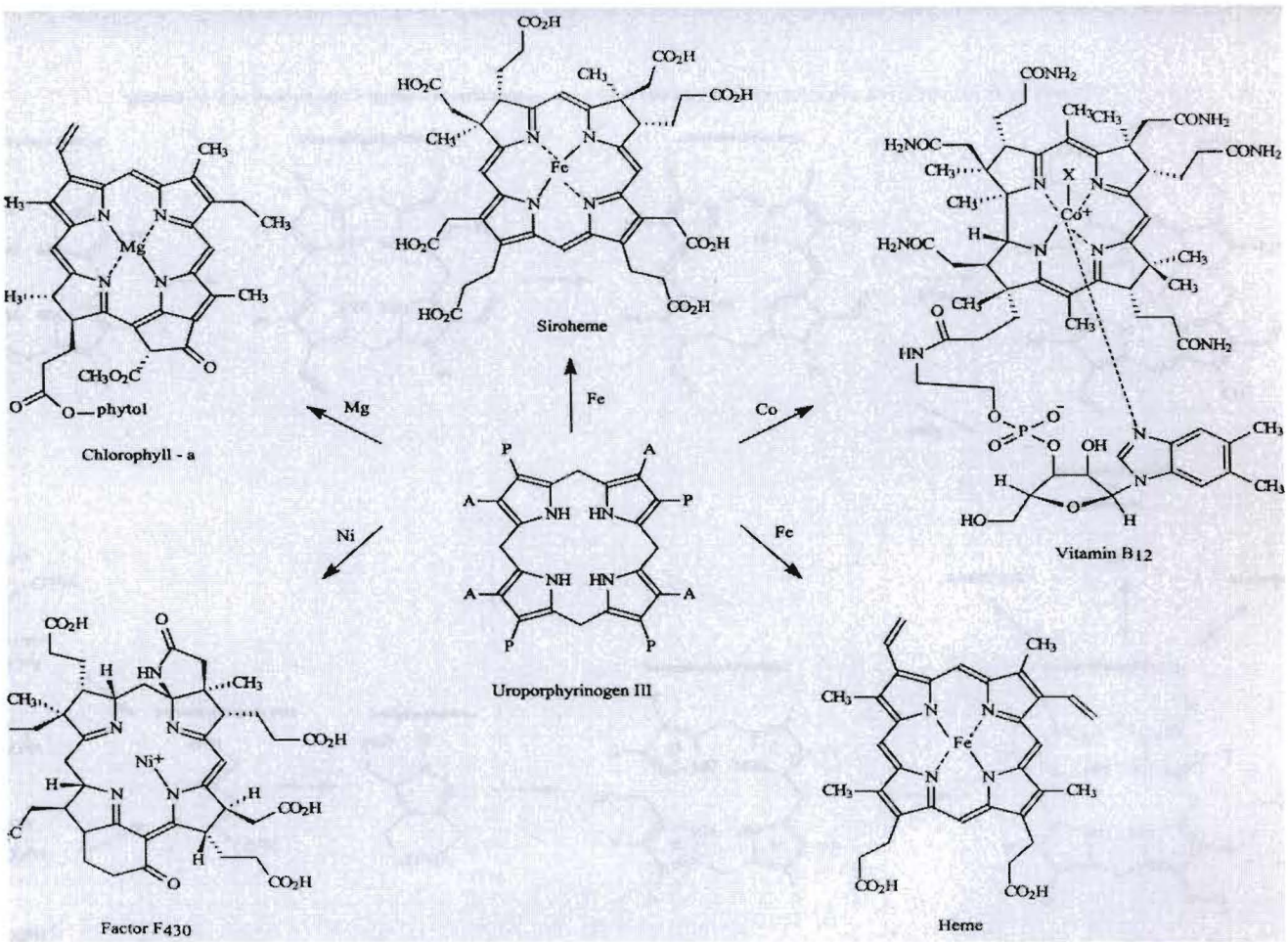

Figure 2. Structures of some important porphobilinogen derivatives. Clockwise from top left is chlorophyll-a, siroheme, vitamin B_{12}, heme, and cofactof F_{430}[11].

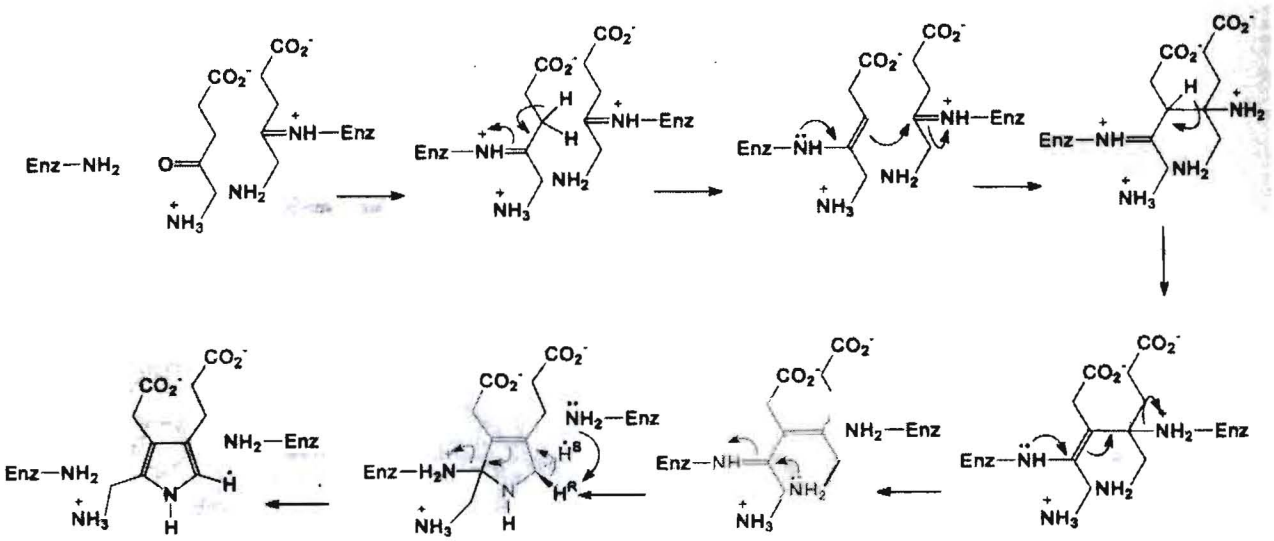

Scheme 3. Mechanism proposed for porphobilinogen synthesis proposed by Jordan et. al. Both substrate molecules are bound to enzyme through Schiff bases and C-C bond is the first one formed[11].

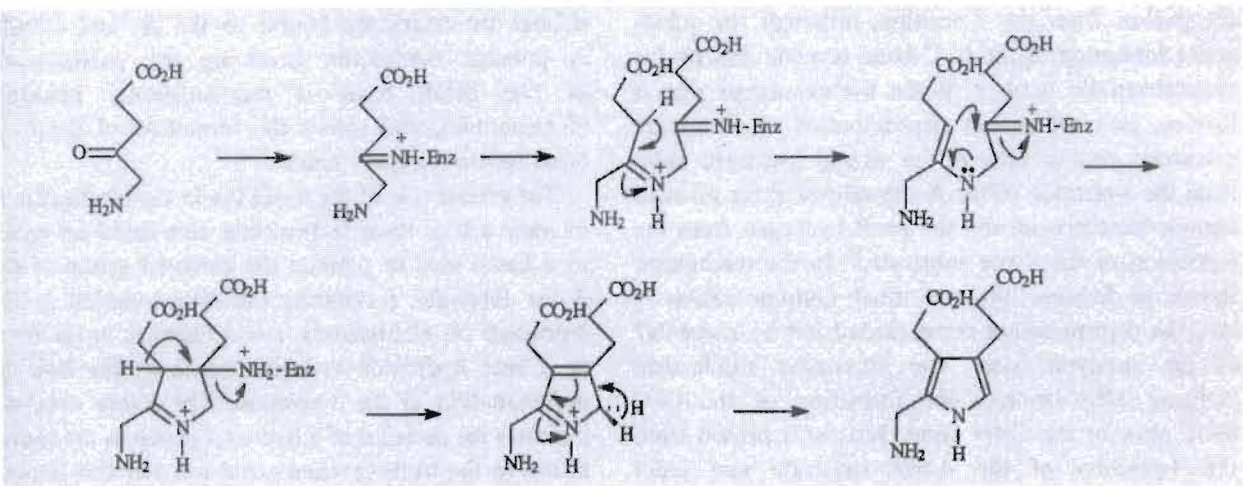

Scheme 4. Alternate mechanism proposed for porphobilinogen synthesis. Only one of the substrate molecules are bound to enzyme through a Schiff base and the C-N bond is the first one formed[11].

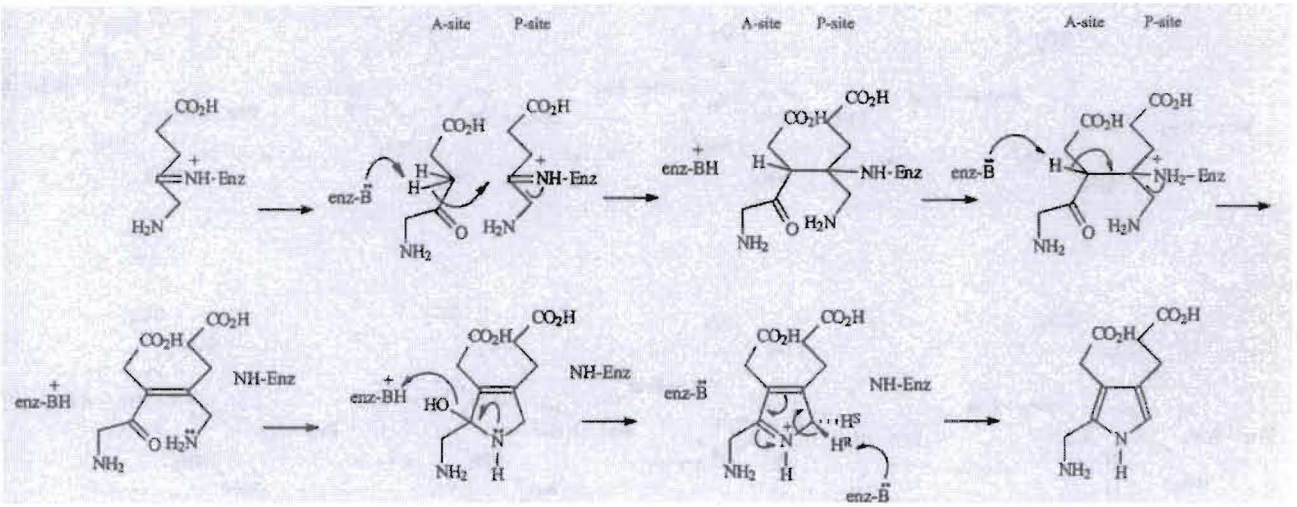

Scheme 5. Alternate mechanism proposed for porphobilinogen synthesis. Only one of the substrate molecules are bound to enzyme through Schiff bases and the C-C bond is the first one formed[11].

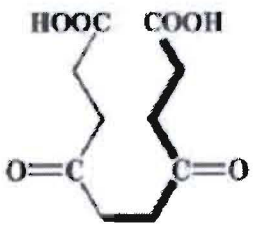

a .)

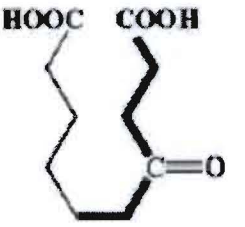

b.)

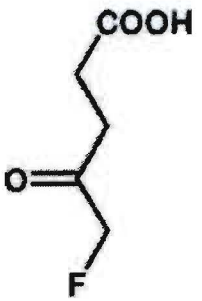

c.)

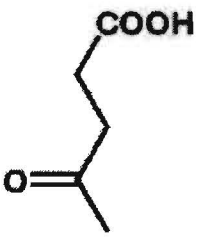

d.)

Figure 6. Inhibitors of PBGS used for inhibition studies to determine the mechanism of PBGS. Clockwise from top left the molecules are: a.) 4,7-dioxosebacic acid; b.) 4-oxosebacic acid; c.) 5-fluorolevulinic acid; 6.) levulinic acid[3,6].

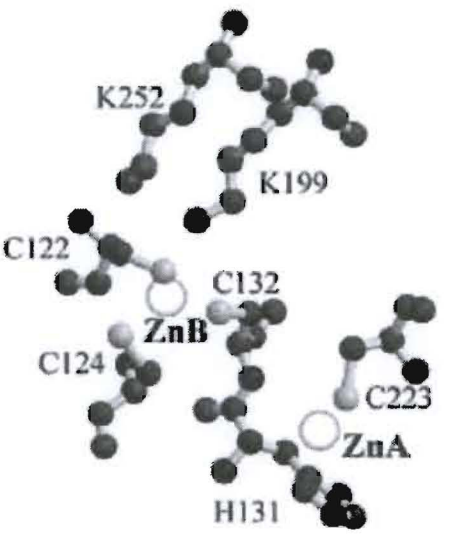

Figure 7. Homology model of two different zinc binding sites (ZnA and ZnB) in the active site of the human PBGS monomer[5].

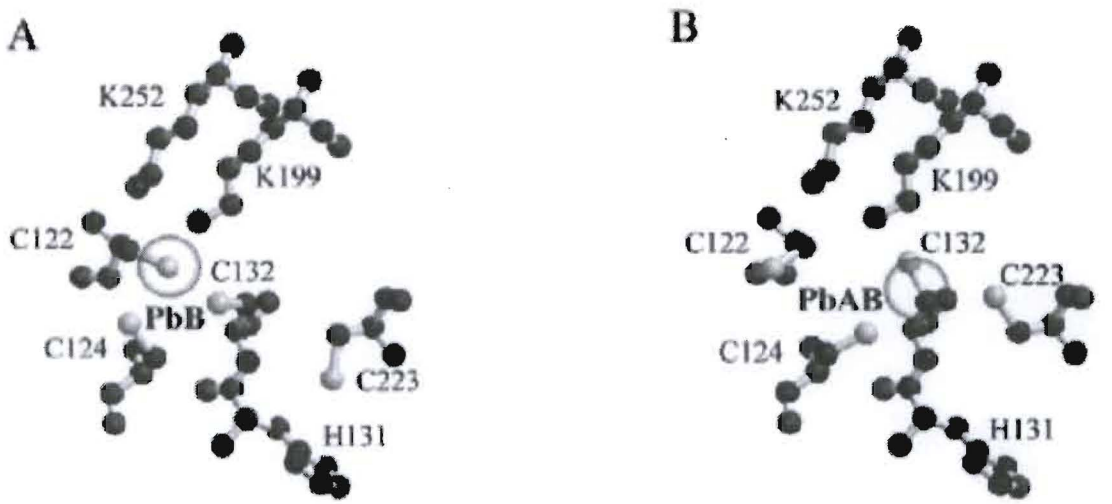

Figure 8. Two models for Pb(II) interaction with human PBGS. A.) models the possibility that Pb(II) is bound to the PbB site (analogous to ZnB site). B.) models the possibility that Pb(II) is bound to the hybrid site PbAB (analogous to a hybrid of the ZnA and ZnB sites)[5].

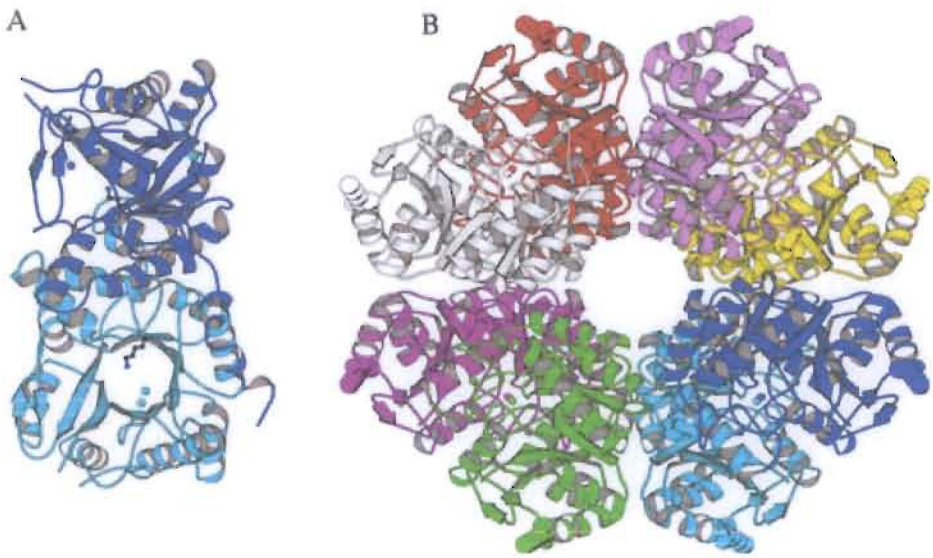

Figure 9. A model for human PBGS based on the crystal structure of yeast PBGS: **A.**) depicts the dimer in the "69" confirmation and **B.**) depicts the octamer[8].

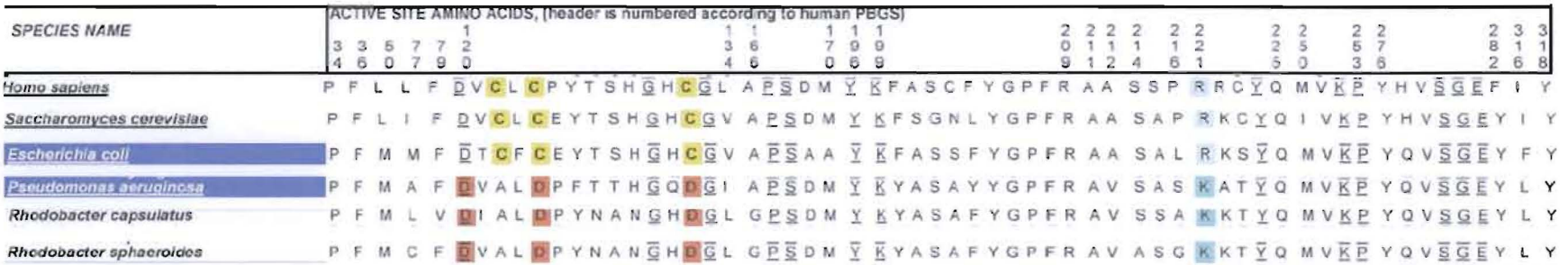

Figure 10. Alignment of amino acid residues considered to be within 8 Å of the active site by the human PBGS (PDB code 1E51). Residues are numbered with respect to the human PBGS sequence. Yellow cysteine residues are ligands to active site zinc. Red aspartate residues form putative metal binding sites that do not use active site zinc. Turquoise lysine residues and light blue arginine residues cosegregate with the absence and presence of active site zinc respectively. Also, species names in dark blue have sequences that indicate a allosteric magnesium binding site[4].

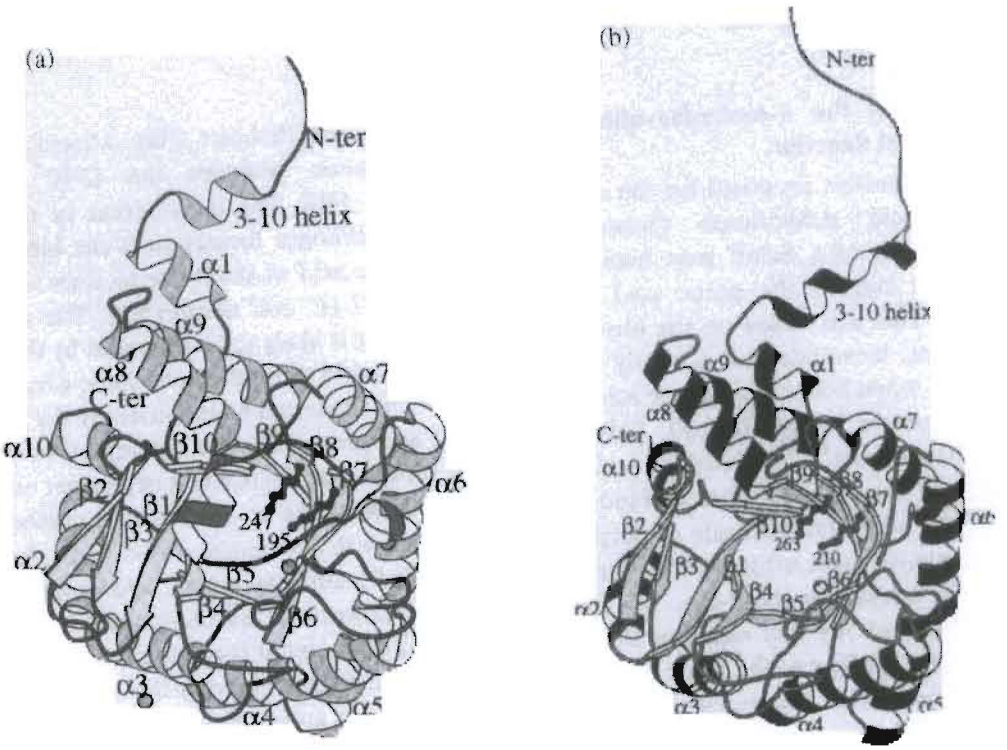

Figure 11. Structure of PBGS monomers from X-ray structures of *E. coli* PBGS. The active site is located in the center of the αβ barrel. The N-terminal arm is also shown[11].

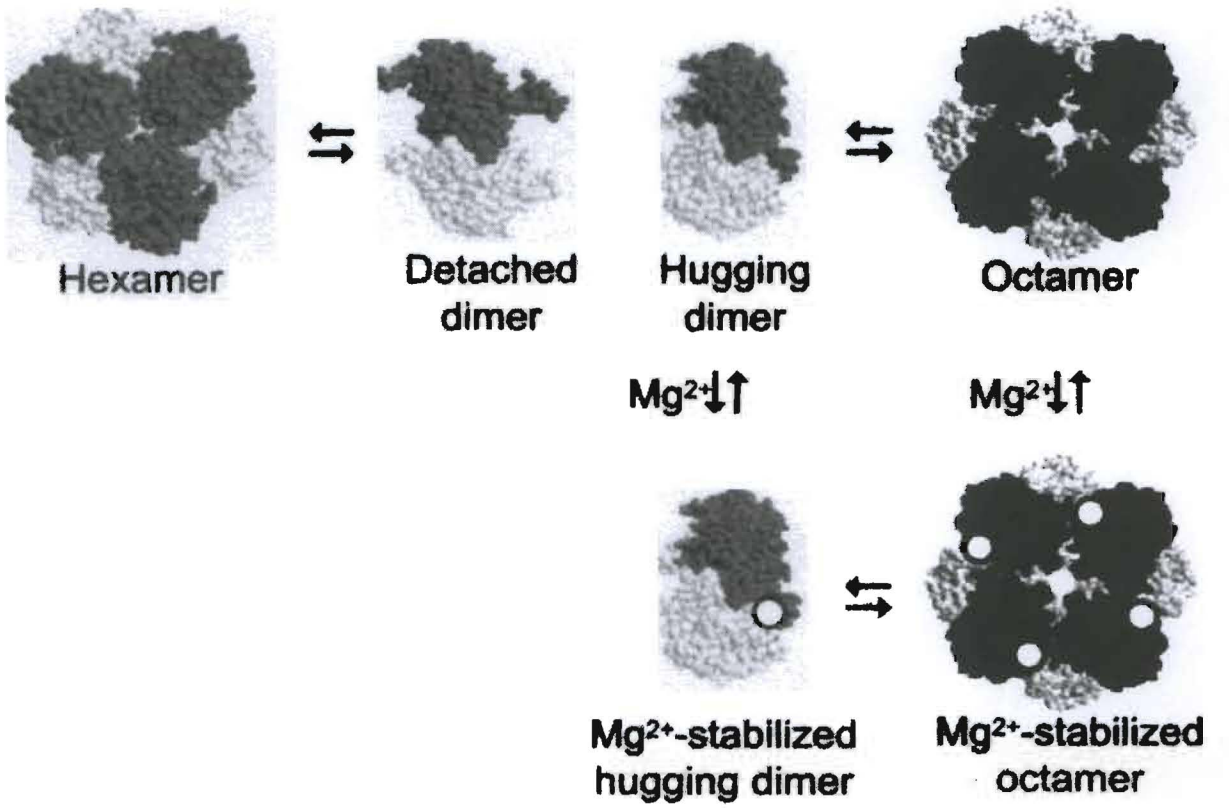

Figure 12. Graphical representation of physiologically relevant interconversion of hexameric and octameric PBGS in an allosteric magnesium containing species .The hexamer can dissociate into detached dimers in a protein concentration-dependent fashion. The detached dimer and hugging dimer are in equilibrium. The hugging dimers can form the octamer, also in a protein concentration-dependent way. Allosteric magnesium stabilizes the hugging dimer and/or octamer structure[2].

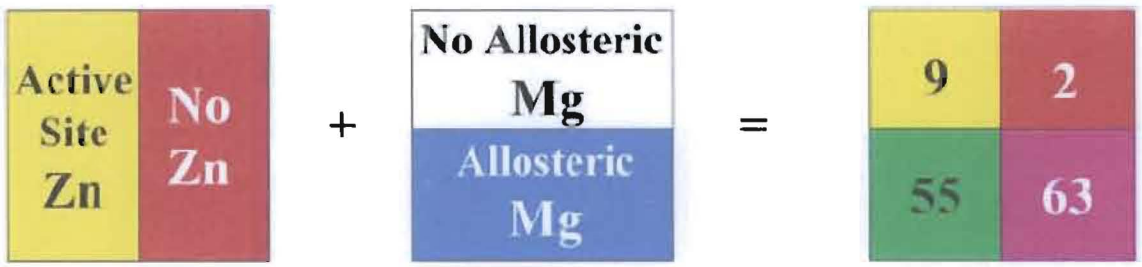

Figure 13. Novel classification scheme for PBGS enzymes. The leftmost square represents the classification on active site metals. The middle square represents the classification based on allosteric site metals. The rightmost square is the numerical breakdown of known PBGS sequences into the four groups created by overlaying the two classifications[3].

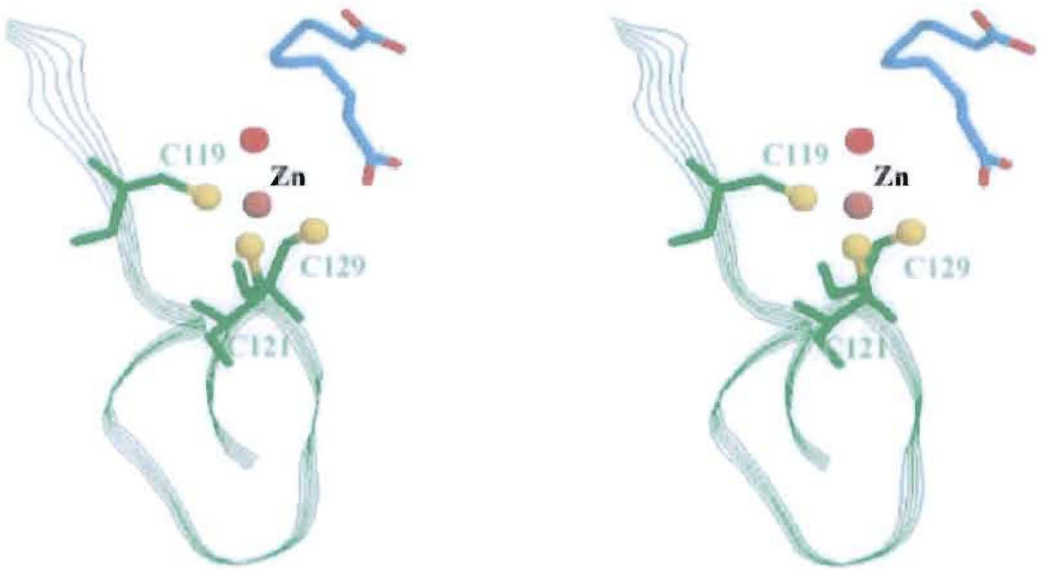

Figure 14. A stereo diagram of *E. coli* PBGS active site. Shows highlighted cysteine residues complexing a Zn^{2+}. Also, a water molecule and an inhibitor molecule are shown over the Zn^{2+} [4].

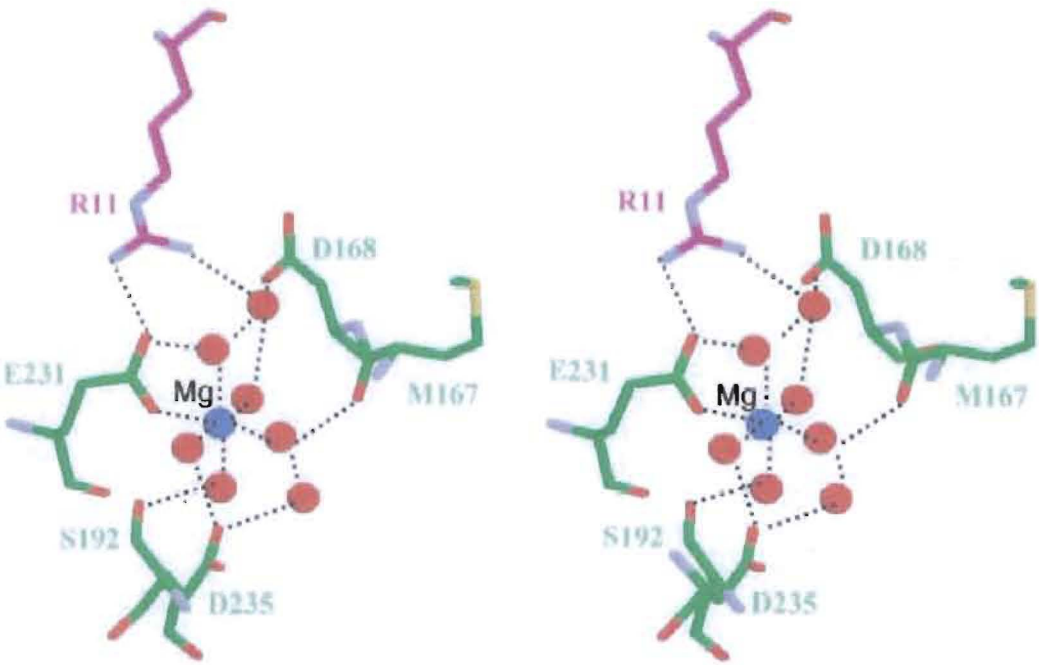

Figure 15. A stereo diagram of the allosteric magnesium binding site of *E. coli* PBGS. Spheres representing water molecules form an extended ligation network around a central Mg^{2+} [4].

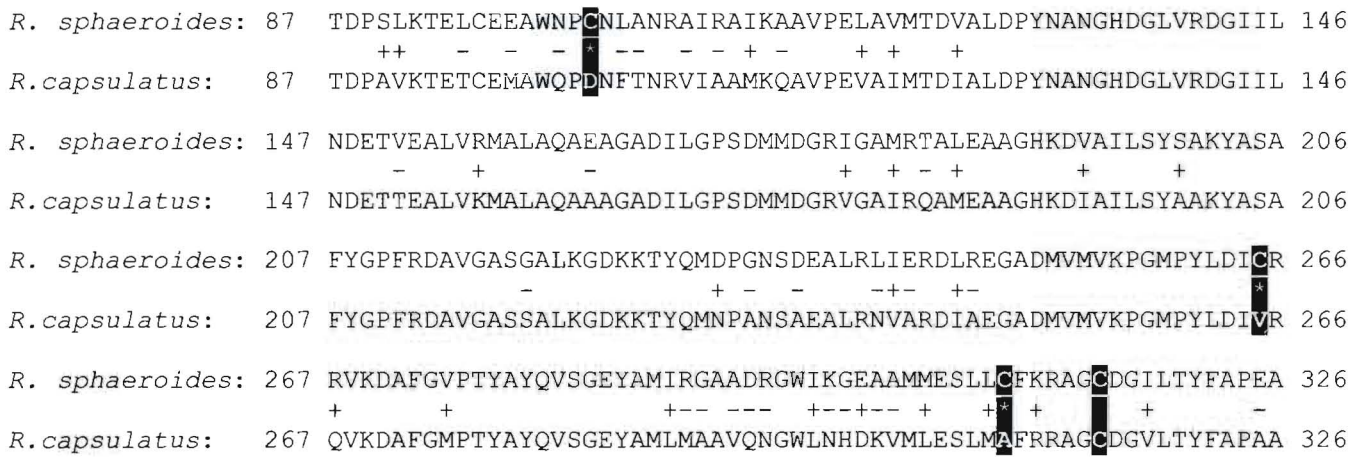

Figure 16. Alignment of *R. capsulatus*[1] and *R. spaeroides*(from http://www.ncbi.nlm.nih.gov/BLAST/). Conservative amino acid residue changes are denoted by a '+' and nonconservative amino acid residue changes are denoted by a '-'. Cysteine residues near the active site are shown with black back grounds, and the active site cysteine residues that are present only in *R. sphaeroides* are marked with an '*'.

Sample	SA w/o β-mercaptoethanol	SA w/ β-mercaptoethanol	Average % Increase in SA	Highest % Increase in SA	Lowest % Increase in SA
C103D	1281.6	1539.5	20.1	33.6	-3.3
C265V	455.3	554.7	21.8	33.7	5.3
C309A	549.3	1053.5	91.8	145.3	64.6
Wild Type	443.9	1191.6	168.4	248.6	114.4

Figure 17. Table of the averages of the specific enzymatic activity of all three mutants and wild type, in the presence and absence of β-mercaptoethanol. Al.so, give average, highest and lowest percent increase in specific activity by β-mecaptoethanol

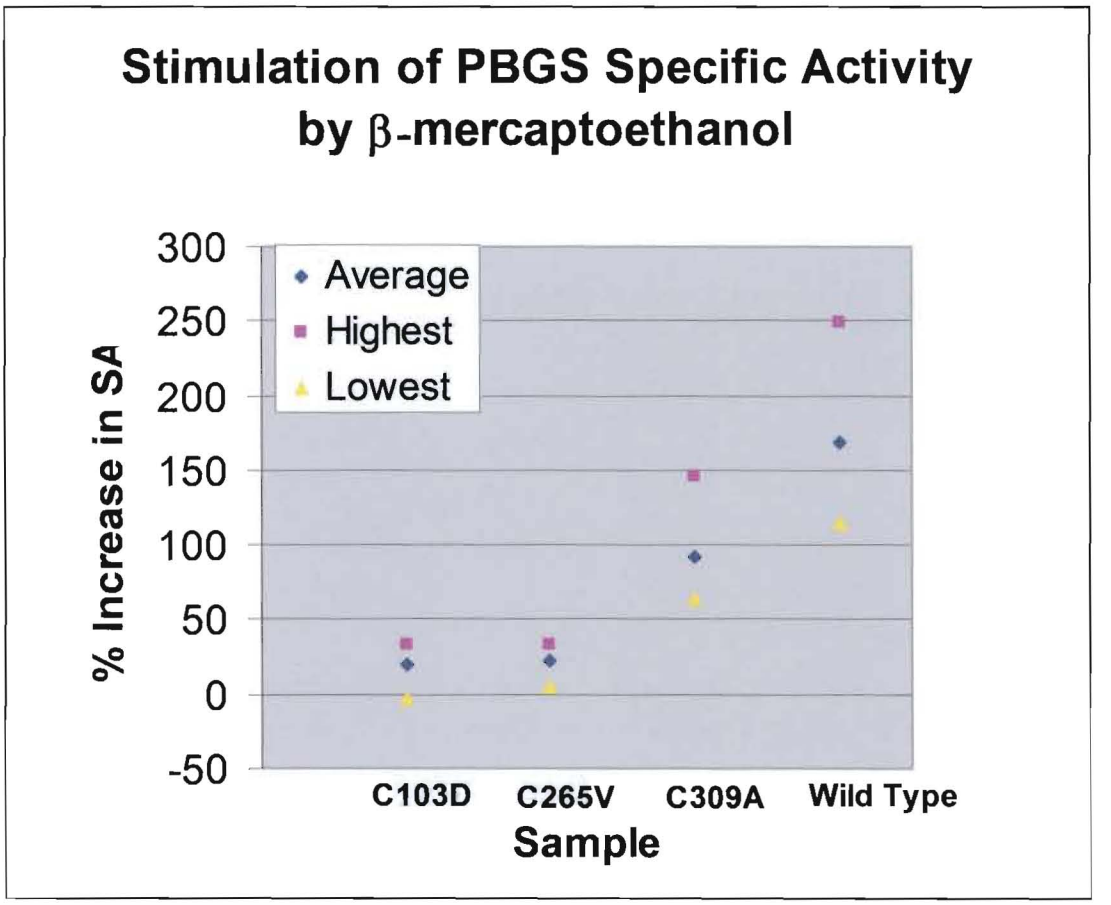

Figure 18. Graph of the the average (blue diamond), highest (pink square), and lowest (yellow triangle) percent decreases in specific activity in each mutant and wild type when activity assays were performed with out β-mercaptoethanol

```
Mutant C103D:  357  ggcctggaaccccgacaacctcgccaaccgg  387
                    ||||||||||||| ||||||||||||||||
R.sphaeroides: 617  ggcctggaaccctgcaacctcgccaaccgg  647
```

Figure 19. Excerpt from sequence alignment between mutant C103D against *R. sphaeroides* (using http://www.ncbi.nlm.nih.gov/BLAST/) done with T7 promoter primer (reads 5′ to 3′). Mismatches are indicated by the lack of a vertical bar between the two bases.

```
Mutant C256V:  227 gcgtccttcacccgccggacgatgtcgagataggg 262
                  ||||||||||||||||||  ||||||||||||||||
R.sphaeroides:1161 gcgtccttcacccgccggcagatgtcgagataggg 1077
```

Figure 20. Excerpt from sequence alignment between mutant C256V against *R. sphaeroides* (using http://www.ncbi.nlm.nih.gov/BLAST/) from terminator primer (reads 3' to 5'). Mismatches are indicated by the lack of a vertical bar between the two bases.